MĀPAN-Journal of Metrology Society of India
https://doi.org/10.1007/s12647-019-00306-y

ORIGINAL PAPER

Pressure Uncertainty Analysis for Wound Irrigation Devices

A. Pawar and T. L. Schmitz*

Department of Mechanical Engineering and Engineering Science, University of North Carolina at Charlotte, Charlotte, NC, USA

Received: 25 January 2019 / Accepted: 07 February 2019

© Metrology Society of India 2019

Abstract: Wound irrigation is defined as the steady flow of a fluid across an open wound for the removal of bacteria, necrotic tissue, and deeper debris. In a wound irrigation process, the surface pressure obtained at the wound is critical. Correct pressure determination ensures that the pressure at the wound due to an irrigation device is enough for the removal of bacteria and foreign debris, but not so high that it causes further tissue damage. Surface pressure measurements were performed for three irrigation devices, including a 500-ml bottle with four holes in the pouring cap, a 60-ml Monoject^{TM} COVIDIEN^{TM} syringe, and an IRIG-8^{TM} Wound Irrigation System from CENTURION^{TM}. The irrigation trials were performed by a total of 20 participants consisting of doctors and nurses using the three devices (60 trials) at the Carolina Medical Center Emergency Department, Charlotte, NC. The uncertainty in the pressure measurements was evaluated using both Monte Carlo and analytical approaches, and the results are reported. It is anticipated that this study will help to standardize irrigation pressure measurement within the medical community.

Keywords: Wound irrigation; Pressure; Uncertainty; Monte Carlo

1. Introduction

Each year there are millions of emergency department visits for wound treatment in the USA [1]. Proper wound management is essential to prevent infection and ensure better and faster healing [2]. Rapid healing is best accomplished by providing an optimized environment [3]. Wound irrigation is one of the most important features of wound management [4] and is widely accepted as one of the best methods for wound cleansing [5].

Wound irrigation is defined as the steady flow of a fluid across an open wound for the removal of bacteria, necrotic tissue, and deeper debris [6]. It also helps in visual inspection of the wound by identifying source of bleeding and determining if there is an emergency surgical concern [2]. There are different methods of irrigating a wound. Traditionally, devices such as bulb syringes, syringes with an attached needle, and a plastic container with a cap or nozzle have been used to deliver the irrigation fluid to the wound. The medical devices presently used are designed to provide a steadier wound pressure [2]. The three key factors that influence the efficiency of wound irrigation are irrigation pressure, volume, and solution. Of these, the irrigation solution is less important than the other two [7]. According to Mittra et al. [8], irrigation pressure is the most important wound irrigation factor. Surface pressure lower than the ideal will not be sufficient for bacterial removal. Also, pressure higher than the ideal can cause tissue damage and increase the potential for further contamination [8].

High pressure irrigation has been widely described as an important aspect of effective wound irrigation. However, the required pressure has not been standardized within the medical community. According to Wedmore et al. [9], irrigation pressure between 103 and 172 kPa (15 psi and 25 psi) constitutes high pressure irrigation. In another study, high pressure irrigation was defined from 34.5 to 55.2 kPa (5–8 psi) [10]. Singer et al. [3] identified pressure greater than 48.3 kPa (7 psi) as high pressure irrigation. Determining the actual wound surface pressure is required to standardize "high pressure" irrigation.

A research study completed by Nicks et al. [2] points out a lack of substantial literature regarding the deliverable irrigation pressure, with many studies failing to measure the actual pressure. Nicks et al. [2] also note that many studies failed to describe the method used for measurement of the wound pressure. Studies that do describe a method of

*Corresponding author, E-mail: tony.schmitz@uncc.edu

Published online: 07 March 2019

measurement have done so using different models for the irrigation pressure measurement. A standard method with the evaluation of the measurement uncertainty is required to improve understanding of irrigation pressure.

Classically, Bernoulli's equation was used to measure the impact pressure at the wound area. A study by Mittra et al. [8] showed that the values obtained from Bernoulli's equation differ from the actual wound surface impact pressure and, therefore, it does not offer an effective wound pressure measurement. This is due to assumptions including steady, incompressible, one dimensional, and laminar flow. Mittra et al. [8] measured the pressure by directing the stream from the irrigation device on a metal beam. Bending of the beam deflected a laser onto a calibrated wall scale. However, Mittra et al. [8] did not measure the actual impact area, but rather assumed that the cross-sectional area of the impact stream was equal to the cross-sectional area of the respective exit lumen. Another limitation of this study was that it took place in a controlled environment and, therefore, did not represent a clinical setting. Also, pressure measurement was a secondary purpose in this study.

In a study by Singer et al. [4], two inline Transpac® IV Disposable pressure transducers were used along with other setup for measuring wound pressure using various irrigation devices. However, as noted by Singer et al. [4], since measurement in an open system is complex, the pressure transducers measured pressure in a closed system. Hence, the actual surface wound pressure was not measured in these trials.

Here, surface wound pressure was calculated from measurements of: (1) the fluid stream force at the point of impact and (2) the cross-sectional area of the fluid at the same location. The force was measured by a piezoelectric force sensor; force data filtering was implemented in MATLAB R2017a. The stream's cross-sectional area was calculated by using Canny edge detection in MATLAB R2017a to locate the fluid stream edges and, therefore, the fluid stream diameter. An uncertainty analysis was performed to evaluate the pressure measurement uncertainty. Based on the literature survey, this pressure measurement has not been previously implemented and offers a first step in standardizing wound surface pressure measurement in clinical environments. The pressure calculation was completed for 20 participants using three different irrigation devices: a 500-ml bottle with four holes in the pouring cap, a 60-ml Syringe Monoject™ COVIDIEN™ syringe, and a Sterile IRIG-8™ Wound Irrigation System from CENTURION™. The duration of each of the 60 trials was also recorded. This duration was the time to administer 500 ml of fluid to the target area.

2. Methodology

A setup was designed to perform the pressure measurements and subsequent data analysis. This setup included a 3D printed target (a post that represented the wound area), containers (to catch the fluid after impact), a Kistler MiniDyn force dynamometer, and a digital single-lens reflex (DSLR) camera to photograph the stream image during fluid application. See Figs. 1 and 2.

Surface wound pressure was calculated from measurements of: (1) the fluid stream force at the point of impact and (2) the cross-sectional area of the fluid at the same location. This location was selected because the stream diameter varied between the device and target surface, in general. The impact force was measured by the dynamometer, while the impact area was determined from the camera images and subsequent image processing in MATLAB R2017a.

Time domain force data for all 60 trials was also analyzed in MATLAB. Measured z direction force data for a single trial using the 60-ml syringe is shown in Fig. 3 (top panel). Electrical noise was present in the measured data as well as drift and a DC offset. A third-order low-pass Butterworth filter with a cutoff frequency of 1 Hz was used to attenuate high frequency noise. Drift compensation was completed by finding the slope of the line passing through the fluid impact start time and end time and then subtracting that line from the force data set. Noise filtering, slope removal, and DC offset removal were completed for the measured force in all three directions separately (F_x, F_y, and F_z). The components were then combined vectorially to obtain the resultant force (F). The same process was followed for all 60 trials.

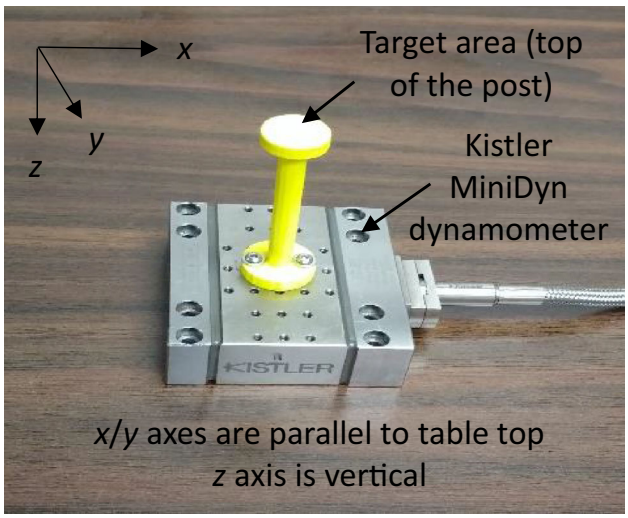

Fig. 1 Target and dynamometer setup

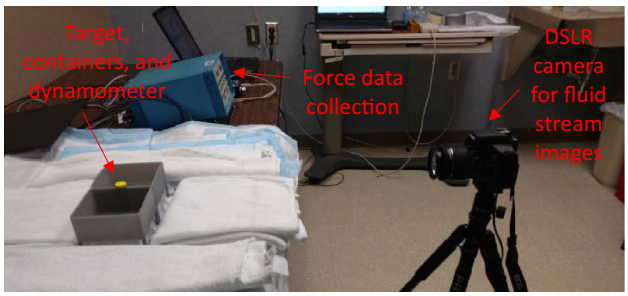

Fig. 2 Photograph of the experimental setup

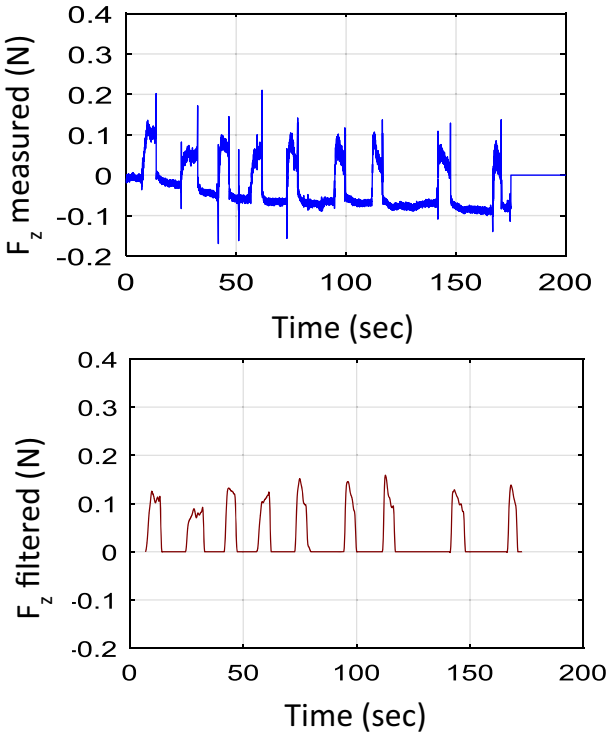

Fig. 3 Time domain force data (F_z) for participant 13. (Top) measured, (bottom) filtered

The cross-sectional impact area of the fluid stream was estimated by locating the edges of the stream close to the point of impact from its digital image captured during fluid application. The distance between the edges provided the diameter of the impact area which, in turn, was converted into the cross-sectional area of the fluid. The Canny edge detection algorithm was applied in this study. An edge detection example using the 60-ml syringe is shown in Fig. 4.

The time-dependent fluid stream pressure was calculated by dividing the time-dependent force by the total stream impact area. This was done for each participant using all three irrigation devices. Also, an uncertainty analysis was

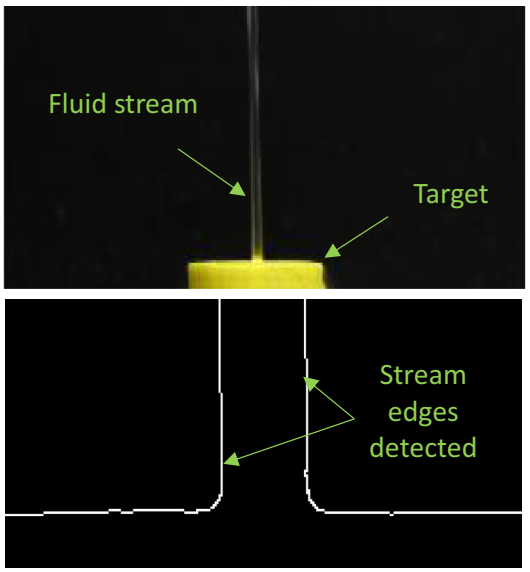

Fig. 4 Edge detection for participant 13 using the 60-ml syringe. (Top) image, (bottom) result

completed to evaluate the measured pressure uncertainty for each trial.

3. Uncertainty analysis

Every measurement result has an associated uncertainty. It is essential to evaluate this uncertainty to fully describe the measurement result. By the law of propagation of uncertainty, the combined standard uncertainty of the dependent variable, or measurand (fluid stream pressure in this case), can be determined analytically by combining the uncertainties in the independent variables (force due to fluid impact and total stream impact area). Equations 1–3 show the pressure equations for the three irrigation devices, where P_i is the time-dependent fluid stream pressure, A_i is the total impact area of the fluid stream(s), F_i is the time-dependent force, p_D is the average pixel count of the post top between edges, p_{di} is the average pixel count of the impact stream, D is the diameter of the post top/target area, and i = 1 (bottle with four holes in the cap, but two streams due to merging of the flow from the four holes), 2 (syringe with a single stream), and 3 (pressurized irrigation system with five holes and five streams).

$$P_1 = \frac{F_1}{A_1} = \frac{F_1}{2\pi\left(\frac{Dp_{d1}}{2p_D}\right)^2} = \frac{2F_1 p_D^2}{\pi D^2 p_{d1}^2} \tag{1}$$

$$P_2 = \frac{F_2}{A_2} = \frac{F_2}{\pi\left(\frac{Dp_{d2}}{2p_D}\right)^2} = \frac{4F_2 p_D^2}{\pi D^2 p_{d2}^2} \tag{2}$$

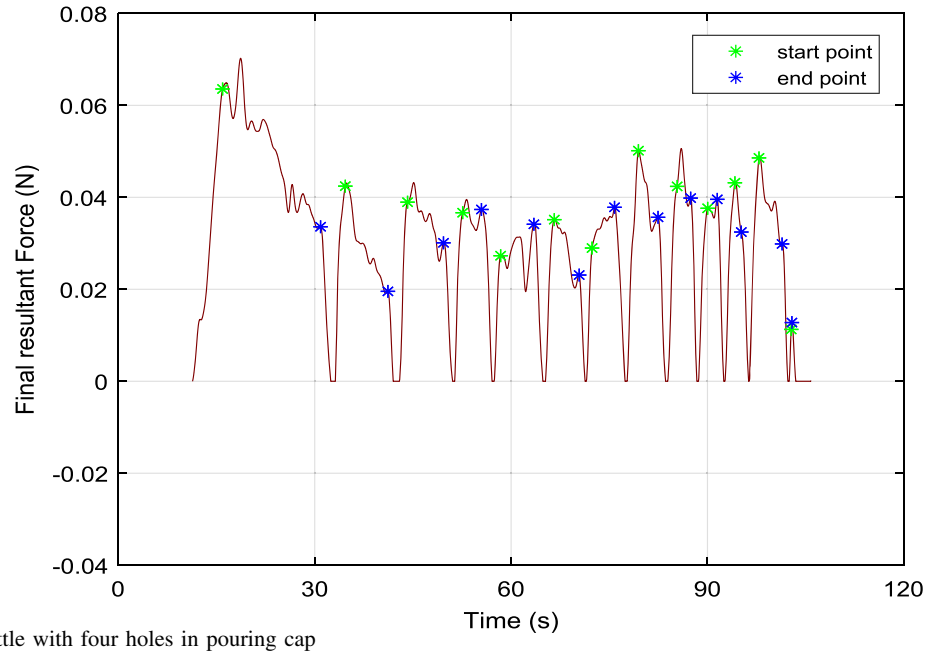

Fig. 5 Force for bottle with four holes in pouring cap

$$P_3 = \frac{F_3}{A_3} = \frac{F_3}{5\pi\left(\frac{Dp_{d3}}{2p_D}\right)^2} = \frac{4F_3p_D^2}{5\pi D^2 p_{d3}^2} \tag{3}$$

As per GUM [11, 12], the combined standard uncertainty of a measurand (which is influenced by input variable uncertainties) is described as the square root of the sum of the products of squares of the input uncertainties and the squares of the sensitivity coefficients (i.e., partial derivative of the measurand with respect to the selected input). See Eq. 4, where u_c is the combined standard uncertainty, c_i is a sensitivity coefficient, u_i is an input standard uncertainty, and the correlation between input variables has been taken to be zero. Therefore, to find the combined standard uncertainty the sensitivity coefficients and the standard uncertainties needed to be determined.

$$u_c = \sqrt{\sum_i c_i^2 u_i^2} \tag{4}$$

The sensitivity coefficients were evaluated at the mean pressure for each measurement. The method for calculating the mean values of the input quantities (F, D, p_D, p_d) is described in the following paragraphs.

For F, the following steps were used. First, the time interval for the applied pressure was determined. For the pressurized device, there was a single interval per trial. For the bottle and syringe, however, there were multiple intervals (to reach the distributed volume of 500 ml). In all cases, the interval was identified by two points based on the start and end points (Fig. 5 shows an example for the bottle with four holes). The force data for the interval were truncated to contain only force data between these start and end points. The mean force value of the trial was then calculated by taking the mean value of the truncated force data.

The diameter of the post top (D) was measured using a digital Vernier calliper (Mitutoyo CD-6 ASX). This was taken as the mean value. From the post diameter image, the number of pixels between the edges of the post top diameter, p_D, was taken as the mean value. The mean value of p_d was found by counting the number of pixels between the edges of the fluid stream near the impact location or by calculating the average number of pixels in the case of multiple fluid streams.

The sensitivity coefficients, c_i, were determined by calculating the partial derivatives of the measurand (P in this case) with respect to the input quantities: F, D, p_D, and p_d. For the bottle with four holes in the pouring cap, the sensitivity coefficients were calculated using Eqs. 5–8.

$$\frac{\partial P_1}{\partial F_1} = \frac{2p_D^2}{\pi D^2 p_{d1}^2} \tag{5}$$

$$\frac{\partial P_1}{\partial D} = -\frac{4F_1p_D^2}{\pi D^3 p_{d1}^2} \tag{6}$$

$$\frac{\partial P_1}{\partial p_D} = \frac{4F_1p_D}{\pi D^2 p_{d1}^2} \tag{7}$$

$$\frac{\partial P_1}{\partial p_{d1}} = -\frac{4F_1p_D^2}{\pi D^2 p_{d1}^3} \tag{8}$$

Similarly, the sensitivity coefficients were calculated for the syringe device and the pressurized irrigation device by

taking the partial derivatives of P with respect to the corresponding input quantities (F, D, p_D, p_d).

The standard uncertainties were set equal to the standard deviations of the corresponding inputs: F, D, p_D, and p_d. The uncertainty in F was calculated form the noise floor of the force data. The force data were truncated between the start of the sampling time and the start of the force interval. The standard deviation of these values was calculated and taken to be the uncertainty in F.

The uncertainty in D was obtained from the specifications for the digital calliper since it was used for the measurement of the diameter of the post top (target area). The value represented as "accuracy" by the manufacturer was taken to be the standard uncertainty in D.

The uncertainty in p_D was determined by calculating the pixel count of 10 rows of values between post top edges at the impact point of the stream. The standard deviation of the 10 adjacent pixel count values was taken as the standard uncertainty.

Similarly, the uncertainty in p_d was determined by calculating the pixel count of 10 rows of values as close as possible to the impact point of the stream. The standard deviation of the 10 adjacent pixel count values was taken as the standard uncertainty.

Substituting the sensitivity coefficient expressions and the standard uncertainties, the combined standard uncertainty can be written as shown in Eq. 9. The expanded uncertainty, U, was obtained by multiplying the combined standard uncertainty by a coverage factor, k. A coverage factor of 2 was selected here; see Eq. 10. Using Eq. 10, the expanded uncertainty values for the 20 participants using the three irrigation devices were calculated.

$$u_c(P) = \left(\left(\frac{\partial P}{\partial F}\right)^2 u^2(F) + \left(\frac{\partial P}{\partial D}\right)^2 u^2(D) + \left(\frac{\partial P}{\partial p_D}\right)^2 u^2(p_D) + \left(\frac{\partial P}{\partial p_d}\right)^2 u^2(p_d) \right)^{0.5} \quad (9)$$

$$U(P) = k u_c(P) \quad (10)$$

Alternately, Monte Carlo simulation [13] may be applied to evaluate the pressure measurement uncertainty. In this case, the measurand uncertainty is evaluated by:

1. Defining the relationship between the inputs and outputs: in this case the pressure expressions are defined by Eqs. 1–3 for the three irrigation devices using four inputs: force, pixel count for the post/target, pixel count for the fluid stream near the impact location, and the post/target diameter
2. Defining the input distributions: normal distributions (with a standard deviation equal to the standard uncertainty) were assumed for each input in this analysis
3. Randomly sampling from each input distribution to calculate one possible output
4. Repeating this process many times to obtain the output distribution.

Table 1 Input values for Monte Carlo and analytical analysis comparison

F_1 (N)	p_D (pixels)	p_{d1} (pixels)	D (m)
Mean values			
0.041	562	34.3	0.03052
Standard uncertainties			
0.0008	0.82	0.28	5.1×10^{-5}

To demonstrate the Monte Carlo approach and compare the uncertainty with the analytical GUM approach, the measurement data from one participant using the bottle with four holes are provided in Table 1. The mean values and standard uncertainties for the force, F_1, pixel count for the post/target, p_D, pixel count for the fluid stream near the impact location, p_{d1}, and the post/target diameter, D, were determined as described previously.

Using Eq. 1, the mean value of the pressure, P_1, is 7.523 kPa. The combined standard uncertainty obtained from Eqs. 5–9 is 194.3 kPa. Figure 6 displays the histogram for the P_1 distribution from 1×10^6 Monte Carlo[1] iterations (100 bins was selected for plotting purposes). The mean is 7.524 kP, and the standard deviation is 194.3 kPa. This level of agreement between the Monte Carlo and analytical approaches was observed for all cases.

4. Results

Figure 7 shows the mean pressure obtained for all 20 participants using the three irrigation devices. The error bars represent the expanded uncertainty ($k = 2$) obtained from the Monte Carlo simulation approach. It is observed that the mean pressure obtained from all participants is the highest for the 60-ml syringe. The bottle with four holes in the pouring cap had the lowest mean pressure. However, the pressure uncertainty for the syringe was also the highest.

Figure 8 displays the mean of all the mean pressures obtained using each irrigation device. It was calculated by taking the mean of the mean pressure for each participant using the selected irrigation device. The error bars represent the mean of the expanded uncertainties.

[Par33] The MATLAB code used to produce Fig. 6 is included in "Appendix" for the interested reader.

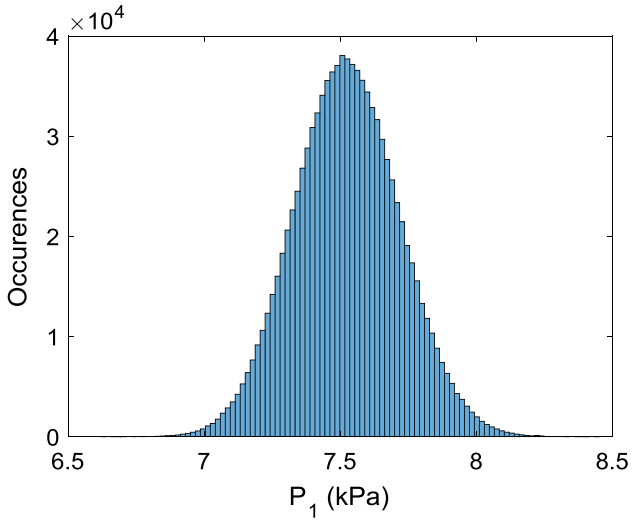

Fig. 6 Histogram (100 bins) for P_1 from Monte Carlo simulation (1×10^6 iterations)

From Fig. 8, the mean pressure of all the participants using an irrigation device was:

- Bottle with four holes in the pouring cap: 10.28 kPa
- Syringe: 80.95 kPa
- Pressurized device: 15.50 kPa.

Figures 9, 10, and 11 show the mean, maximum, and minimum pressures obtained by the participants using the three irrigation devices. The upper and lower endpoints of the error bars represent the maximum and minimum calculated pressure for the selected participant over all intervals in the trial. For the bottle and syringe, there were multiple intervals, so these maximum and minimum values were selected from all intervals in a single trial. For the pressurized device, these values were obtained from the single interval in the trial.

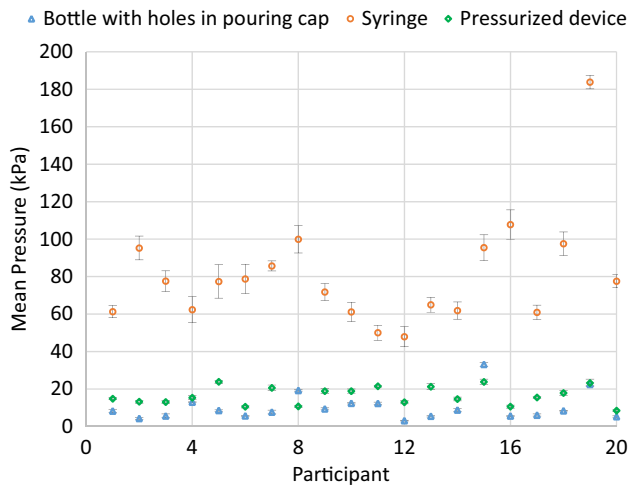

Fig. 7 Mean pressure for all participants with expanded uncertainty ($k = 2$) error bars

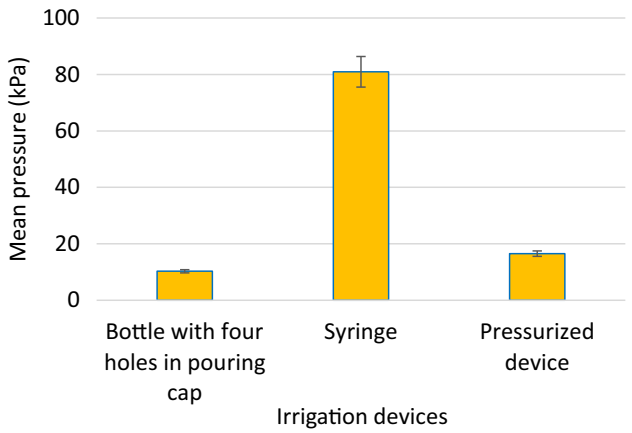

Fig. 8 Mean pressure of all participants with mean expanded uncertainty for the three irrigation devices

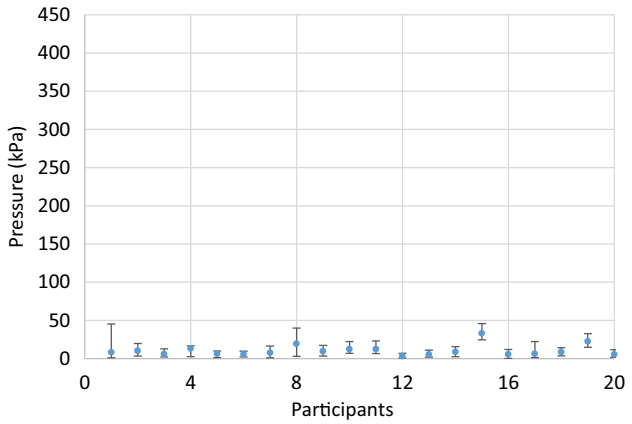

Fig. 9 Mean, maximum, and minimum pressures for all participants using the bottle with four holes in the pouring cap

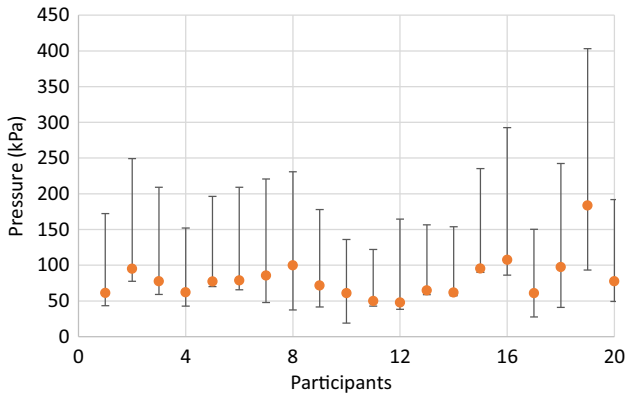

Fig. 10 Mean, maximum, and minimum pressures for all participants using the 60-ml syringe

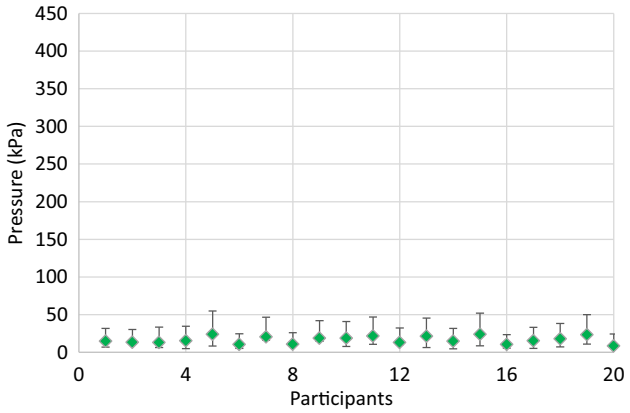

Fig. 11 Mean, maximum, and minimum pressures for all participants using the pressurized device

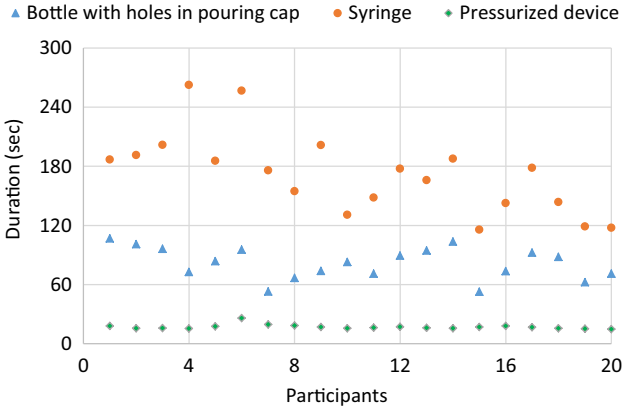

Fig. 13 Duration of each trial for all participants using the three irrigation devices

Figure 12 displays the mean force obtained for all 20 participants using the three irrigation devices. For this result, the total stream area was not considered. Rather, the total impact force was considered only.

Figure 13 displays the duration of each trial for all 20 participants using the three irrigation devices. The trial started when the fluid impacted the target area and ended when the full 500 ml of irrigation fluid was dispensed. The mean duration of a single trial was the highest for the 60-ml syringe. The pressurized irrigation device required the least time and was most consistent.

The mean durations of the trials (i.e., the time taken for a participant to dispense 500 ml using an irrigation device) were:

- bottle with four holes in the pouring cap: 81 s
- syringe: 172 s
- pressurized device: 17 s.

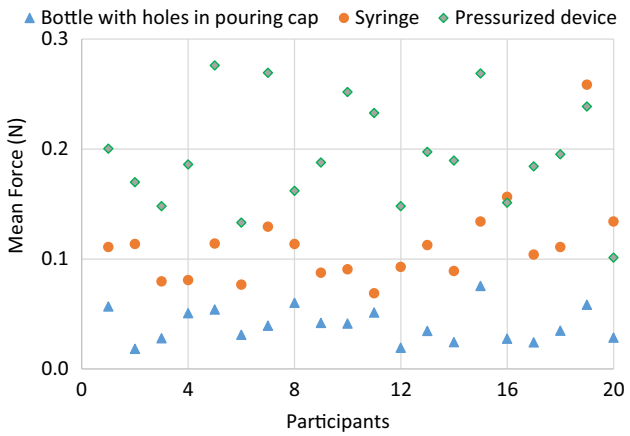

Fig. 12 Mean force for all trials using the three irrigation devices

5. Conclusions

The purpose of this study was to serve the medical community by studying the pressure imposed on wounds by three common irrigation devices, reporting the experimental techniques, and evaluating the measurement uncertainty using both analytical and Monte Carlo approaches. To collect data for the study, 20 doctors and nurses conducted wound irrigation trials using: (1) a bottle with four holes in the pouring cap; (2) a syringe; and (3) a pressurized irrigation device. The motivation for the study was based on a literature review. The current literature does not contain a standard pressure measurement method for wound irrigation. Further, there is no consensus on what pressure is required for proper irrigation. It is anticipated that this study will help to standardize irrigation pressure measurement within the community.

The study results are summarized here. From Fig. 7, it can be observed that the mean pressure obtained from all participants was highest for the 60-ml syringe. The bottle with four holes in the pouring cap had the lowest mean pressure. However, the pressure uncertainty for the syringe was also the highest. Further, the standard deviation of mean pressures from all participants (as shown in Fig. 8) was the highest for the syringe. The pressurized irrigation device had the lowest standard deviation of mean pressures from all participants.

Observing Fig. 13, the mean duration of a single trial (500 ml dispensation of fluid) was the highest for the 60-ml syringe. The pressurized irrigation device required the lowest time. It was also observed that the standard deviation of trial durations is maximum for the 60-ml syringe and minimum for the pressurized irrigation device.

Appendix: MATLAB code used to produce Fig. 6

```
clc
clear
close

% number of Monte Carlo simulation iterations
points = 1e6;

% mean values of input parameters (selected participant, bottle)
F1m = 0.041;        % measured force, N
pDm = 562;          % pixel count for post/target diameter, pixels
pd1m = 34.3;        % pixel count for stream diameter, pixels
Dm = 30.52e-3;      % measured post/target diameter, m

% standard uncertainties for input parameters
sigma_F1 = 0.0008;  % standard deviation for measured force, N
sigma_pD = 0.82;    % standard deviation for post/target diameter pixel
count, pixels
sigma_pd1 = 0.28;   % standard deviation for stream diameter pixel count,
pixels
sigma_D = 5.1e-5;   % standard deviation for measured post/target diameter, m

% uncertain input parameters
% mean value summed with normal distribution scaled by standard uncertainty
F1 = F1m + sigma_F1*randn(points, 1);
pD = pDm + sigma_pD*randn(points, 1);
pd1 = pd1m + sigma_pd1*randn(points, 1);
D = Dm + sigma_D*randn(points, 1);

% uncertain pressure
P1 = (2*F1.*pD.^2)./(pi*D.^2.*pd1.^2);

figure(1)
histogram(P1/1e3, 100)
set(gca,'FontSize', 14)
xlabel('P_1 (kPa)')
ylabel('Occurences')
xlim([6.5 8.5])
mean(P1)
std(P1)

% compare Monte Carlo results to GUM analytical partial derivative approach
dP1_dF1 = 2*pDm^2/(pi*Dm^2*pd1m^2);
dP1_dpD = 4*F1m*pDm/(pi*Dm^2*pd1m^2);
dP1_dpd1 = -4*F1m*pDm^2/(pi*Dm^2*pd1m^3);
dP1_dD = -4*F1m*pDm^2/(pi*Dm^3*pd1m^2);

P1m = (2*F1m*pDm^2)/(pi*Dm^2*pd1m^2)
uc_P1 = sqrt(dP1_dF1^2*sigma_F1^2 + dP1_dpD^2*sigma_pD^2 +
dP1_dpd1^2*sigma_pd1^2 + dP1_dD^2*sigma_D^2)
```

References

[1] H.G. Skinner, J. Blanchard and A. Elixhauser, Trends in emergency department visits, 2006–2011, Statistical Brief, 179 (2014).

[2] B.A. Nicks, E.A. Ayello, K. Woo, D. Nitzki-George and R.G. Sibbald, Acute wound management: Revisiting the approach to assessment, irrigation, and closure considerations, Int. J. Emerg. Med., **3/4** (2010) 399-407.

[3] A.J. Singer and A.B. Dagum, Current management of acute cutaneous wounds, N. Engl. J. Med., **359/10** (2008) 1037-1046.

[4] A.J. Singer, J.E. Hollander, S. Subramanian, A.K. Malhotra and P.A. Villez, Pressure dynamics of various irrigation techniques commonly used in the emergency department, Ann. Emerg. Med., **24/1** (1994) 36-40.

[5] B.S. Atiyeh, S.A. Dibo and S.N. Hayek, Wound cleansing, topical antiseptics and wound healing, Int. Wound J., **6/6** (2009) 420-430.

[6] W.J. Ennis, W. Valdes, S. Salzman, D. Fishman, and P. Meneses, Trauma and wound care (Chapter 17), M.J. Morison, L.G. Ovington and K. Wilkie, Eds.; Chronic wound care. a problem-based learning approach. London: Mosby Elsevier Limited, pp. 291-307 (2004).

[7] F. Wu and M.E. Winters, Emergency medicine, an issue of physician assistant clinics, E-book, Vol. 2, Elsevier Health Sciences (2017).

[8] E.S. Mittra, A.J. Singer and D. Bluestein, Simulated wound irrigation impact pressures, Isr. J. Emerg. Med., **3** (2003) 9-16.

[9] L.I.S. Wedmore, S.A. Godwin and J.M. Howell, Wound care: modern evidence in the treatment of man's age-old injuries, Emerg. Med. Pract. Em Pract. Guidel. Update, **7/3** (2005) 1-23.
[10] D. Pronchik, C. Barber and S. Rittenhouse, Low-versus high-pressure irrigation techniques in Staphylococcus aureus-inoculated wounds, Am. J. Emerg. Med., **17/2** 1999 121-124.
[11] Evaluation of Measurement Data – Guide to the Expression of Uncertainty in Measurement JCGM 100:2008 (GUM 1995 with minor corrections).
[12] B.N. Taylor and C.E. Kuyatt, Guidelines for evaluating and expressing the uncertainty of NIST measurement results, NIST technical note 1297 (1994).
[13] Evaluation of measurement data—Supplement 1 to the "Guide to the Expression of Uncertainty in Measurement"—Propagation of distributions using a Monte Carlo method JCGM 101:2008.

Publisher's Note Springer Nature remains neutral with regard to jurisdictional claims in published maps and institutional affiliations.